

Remote sensing of backward reflection from stimulated axion decay

Kensuke Homma^{1,2}

¹Graduate School of Advanced Science and Engineering, Hiroshima University, Kagamiyama, Higashi-Hiroshima 739-8526, Japan

²International Center for Quantum-field Measurement Systems for Studies of the Universe and Particles (QUP), KEK, Tsukuba, Ibaraki 305-0801, Japan

(Dated: December 5, 2023)

We propose a method for remotely detecting backward reflection via induced decay of cold dark matter such as axion in the background of a propagating coherent photon field. This method can be particularly useful for probing concentrated dark matter streams by Earth's gravitational lensing effect. Formulae for the stimulated reflection process and the expected sensitivities in local and remote experimental approaches are provided for testing eV scale axion models using broad band lasers. The generic axion-photon coupling is expected to be explorable up to $\mathcal{O}(10^{-12})$ GeV⁻¹ and $\mathcal{O}(10^{-22})$ GeV⁻¹ for the idealized local and remote setups, respectively.

Despite that the topological nature in quantum Chromodynamics (QCD) rather naturally allows CP violation, why is the CP -symmetry conserved in QCD? To resolve this strong CP problem, Peccei and Quinn have proposed the global $U(1)_{PQ}$ symmetry [1, 2]. As a result of the spontaneous PQ-symmetry breaking [3, 4], axion, a hypothetical particle, could appear as a kind of Nambu-Goldstone bosons with non-zero mass. If the energy scale for the symmetry breaking is much higher than that of the electroweak symmetry, the coupling of axion to ordinary matter can be weak. This invisible axion can be a candidate for cold dark matter [5–7]. Typically viable QCD axion models predict its mass much below the eV scale. In contrast, there are several recent models which predict the mass range around eV in the context of astrophobic QCD axion [8, 9] which are motivated to solve the anomalous cooling in several stellar environments [10–12]. Moreover, an axion-like particle (ALP) model relevant to inflation predicts the eV range ALP [13]. Therefore, it is worth testing the eV scale QCD axion and ALP scenarios as in general as possible.

So far any of axion halo scopes have utilized static magnetic fields to induce axion decay via the inverse Primakoff process [14]. A giant magnet is typically not movable and thus it is practically difficult to bring the searching system to a far region in the universe where the axion density might be enhanced compared to the average density. In concrete, a possibility that the dark matter density is locally concentrated by the gravitational lensing from Earth has been evaluated [15]. The study predicts that fine-grained streams of dark matter form the hair-like structure above the surface of Earth and the typical distance to the roots of hairs is estimated as $\sim 10^9$ m from Earth, where the concentration factor to the average density can reach $10^7 - 10^9$ depending on impact parameters of dark matter streams with respect to Earth [15]. If these hair-roots exist around Earth, we may expect that these positions can be stationary with respect to Earth's motion. We are thus led to consider methods for detecting such remote stationary objects.

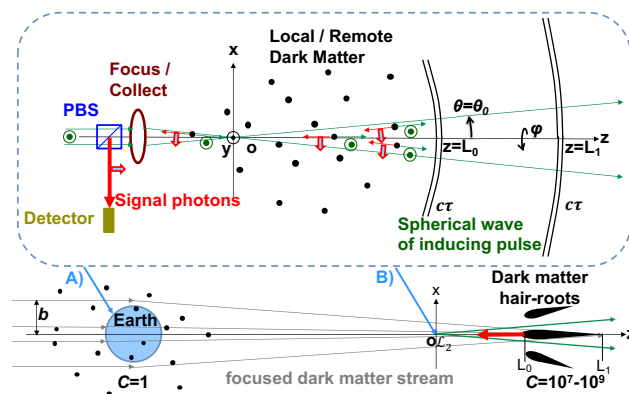


FIG. 1: Concept for detecting backward reflection from stimulated decay of pseudoscalar dark matter such as axion. This concept is applicable to A) laboratory based experiments and B) remote sensing of dark matter hair-roots due to the gravitational lensing effect by Earth with respect to dark matter streams [15]. C expresses the local concentration factor with respect to the average cold dark matter density around the Sun [19]. L_2 corresponds to the Lagrange point where the sun light can be shadowed by Earth. The detailed explanations are found in the main text.

As illustrated in Fig.1 we consider the stimulated decay process of axion in the coherent state into two photons under an inducing photon beam in the coherent state. This process accompanies generation of signal photons with different momenta and polarization states from those of the inducing field in general. However, if axions are non-relativistic and effectively at rest with respect to an observer, due to energy-momentum conservation in the axion's rest frame, the signal photons from stimulated decays must look as if reflection occurs from moving mirrors whose directions are determined by the wave vectors of the inducing photons. Thanks to the reversible nature of focusing and diverging wave vectors in the focused inducing beam, the stimulated emission is expected to be fully collectable at the incident point of the inducing

beam. In addition, since axion is a pseudoscalar particle, the decayed two photons must have the characteristic correlation in the polarization states. If either one photon is in a linearly polarization state, the other one's polarization direction tends to be orthogonal. Therefore, with respect to the polarization direction of the inducing field(y -axis), selecting orthogonally polarized backward photons by a polarization beam splitter (PBS) will help the discrimination from the trivial background process in the search. In the following we formulate this stimulated reflection process and discuss the expected sensitivity to search for pseudoscalar-type dark matter based on local and remote experimental approaches, A) and B), respectively.

We discuss the generic interaction Lagrangian between a pseudoscalar field σ and two photons

$$-\mathcal{L} = gM^{-1}\frac{1}{4}F_{\mu\nu}\tilde{F}^{\mu\nu}\sigma \quad (1)$$

where g is a dimensionless coupling strength and M is an energy scale at which a symmetry breaking occurs with the photon field strength tensor $F_{\mu\nu}$ and its dual tensor $\tilde{F}_{\mu\nu}$ whose definitions are given below. The first order perturbation of S-matrix for the interaction Lagrangian is expressed as

$$S^{(1)} = \left(-\frac{1}{4}\frac{g}{M}\right)\frac{i^1}{1!}\int d^4x N[F_{\mu\nu}(x)\tilde{F}^{\mu\nu}(x)\sigma(x)], \quad (2)$$

where N denotes the normal-ordering of operators with the following Fourier expansions of the relevant fields

$$\sigma(x) \equiv \int \frac{d^3\mathbf{q}}{(2\pi)^3 2q^0} (e^{-iqx} b_{\mathbf{q}} + e^{iqx} b_{\mathbf{q}}^\dagger), \quad (3)$$

$$F^{\mu\nu} \equiv (-i) \int \frac{d^3\mathbf{p}}{(2\pi)^3 2p^0} \Sigma_{\lambda=1,2} (P^{\mu\nu} e^{-ipx} a_{\mathbf{p},\lambda} + \hat{P}^{\mu\nu} e^{ipx} a_{\mathbf{p},\lambda}^\dagger), \quad (4)$$

and

$$\tilde{F}^{\mu\nu} \equiv \frac{1}{2}\varepsilon^{\mu\nu\alpha\beta} F_{\alpha\beta} \quad (5)$$

$$= (-i) \int \frac{d^3\mathbf{p}}{(2\pi)^3 2p^0} \Sigma_{\lambda=1,2} (\tilde{P}^{\mu\nu} e^{-ipx} a_{\mathbf{p},\lambda_p} + \hat{\tilde{P}}^{\mu\nu} e^{ipx} a_{\mathbf{p},\lambda_p}^\dagger),$$

where we introduce the following momentum-polarization tensors as capitalized symbols for an arbitrary four-momentum p of the electromagnetic field with the polarization state λ_p :

$$\begin{aligned} P^{\mu\nu} &\equiv p^\mu e^\nu(\lambda_p) - e^\mu(\lambda_p) p^\nu, \\ \hat{P}^{\mu\nu} &\equiv p^\nu e^{*\mu}(\lambda_p) - e^{*\nu}(\lambda_p) p^\mu, \end{aligned} \quad (6)$$

and

$$\begin{aligned} \tilde{P}^{\mu\nu} &\equiv \frac{1}{2}\varepsilon^{\mu\nu\alpha\beta} (p_\alpha e_\beta(\lambda_p) - e_\alpha(\lambda_p) p_\beta), \\ \hat{\tilde{P}}^{\mu\nu} &\equiv \frac{1}{2}\varepsilon^{\mu\nu\alpha\beta} (p_\alpha e_\beta^*(\lambda_p) - e_\alpha^*(\lambda_p) p_\beta) \end{aligned} \quad (7)$$

with the Levi-Civita symbol ε^{ijkl} . The commutation relations between the photon creation and annihilation operators, $a_{\mathbf{p},\lambda}$ and $a_{\mathbf{p},\lambda}^\dagger$ are as follows

$$\begin{aligned} [a_{\mathbf{k},\lambda}, a_{\mathbf{k}',\lambda'}^\dagger] &= (2\pi)^3 2k^0 \delta^3(\mathbf{k} - \mathbf{k}') \delta(\lambda - \lambda') \quad (8) \\ &\equiv \tilde{\delta}^3(\mathbf{k} - \mathbf{k}') \delta(\lambda - \lambda'), \\ [a_{\mathbf{k},\lambda}, a_{\mathbf{k}',\lambda'}] &= [a_{\mathbf{k},\lambda}^\dagger, a_{\mathbf{k}',\lambda'}^\dagger] = 0. \end{aligned}$$

Henceforth we omit the polarization index λ_p and the sum over it because we require fixed beam polarizations in assumed experiments. Substituting Eqs.(3-7) into Eq.(2), we get

$$S^{(1)} = \left(-\frac{1}{4}\frac{g}{M}\right)\frac{i^1}{1}\int d^4x (-i)^2 \times \quad (9)$$

$$\begin{aligned} &\int \frac{d^3\mathbf{s}}{(2\pi)^3 2s^0} \int \frac{d^3\mathbf{t}}{(2\pi)^3 2t^0} \int \frac{d^3\mathbf{u}}{(2\pi)^3 2u^0} \times \\ &N[(S_{\mu\nu}\tilde{T}^{\mu\nu} e^{-i(s+t)x} a_{\mathbf{s}} a_{\mathbf{t}} + S_{\mu\nu}\hat{\tilde{T}}^{\mu\nu} e^{-i(s-t)x} a_{\mathbf{s}} a_{\mathbf{t}}^\dagger + \\ &\hat{S}_{\rho\sigma}\tilde{T}^{\rho\sigma} e^{-i(t-s)x} a_{\mathbf{s}}^\dagger a_{\mathbf{t}} + \hat{S}_{\rho\sigma}\hat{\tilde{T}}^{\rho\sigma} e^{i(s+t)x} a_{\mathbf{s}}^\dagger a_{\mathbf{t}}^\dagger) \\ &\times (e^{-iu\mathbf{x}} b_{\mathbf{u}} + e^{iu\mathbf{x}} b_{\mathbf{u}}^\dagger)] \end{aligned}$$

where four momenta s , t and u correspond to those in $F^{\mu\nu}$, $\tilde{F}^{\mu\nu}$ and σ , respectively.

The definitions of the coherent state [16] for a given mean number of photons $N_{\mathbf{p}}$ with a three dimensional momentum \mathbf{p} are summarized as follows:

$$|N_{\mathbf{p}}\rangle \equiv \exp(-N_{\mathbf{p}}/2) \sum_{n=0}^{\infty} \frac{N_{\mathbf{p}}^{n/2}}{\sqrt{n!}} |n_{\mathbf{p}}\rangle, \quad (10)$$

where $|n_{\mathbf{p}}\rangle$ is the normalized state of n photons

$$|n_{\mathbf{p}}\rangle = \frac{1}{\sqrt{n!}} (a_{\mathbf{p}}^\dagger)^n |0\rangle, \quad (11)$$

with the creation operator $a_{\mathbf{p}}^\dagger$ of photons that share a common momentum \mathbf{p} and a common polarization state over different number states. The following relations on the coherent state

$$\langle\langle N_{\mathbf{p}}|N_{\mathbf{p}}\rangle\rangle = 1 \quad (12)$$

and

$$\langle\langle N_{\mathbf{p}}|n|N_{\mathbf{p}}\rangle\rangle = \langle\langle N_{\mathbf{p}}|(a_{\mathbf{p}}^\dagger)^n|N_{\mathbf{p}}\rangle\rangle = N_{\mathbf{p}}, \quad (13)$$

give us basic properties with respect to the creation and annihilation operators to the coherent state:

$$a_{\mathbf{p}}|N_{\mathbf{p}}\rangle = \sqrt{N_{\mathbf{p}}}|N_{\mathbf{p}}\rangle, \quad \text{and} \quad \langle\langle N_{\mathbf{p}}|a_{\mathbf{p}}^\dagger = \sqrt{N_{\mathbf{p}}}\langle\langle N_{\mathbf{p}}|. \quad (14)$$

For the coherent state of a pseudoscalar field we apply the same properties to the annihilation and creation operators $b_{\mathbf{p}}$ and $b_{\mathbf{p}}^\dagger$, respectively,

$$b_{\mathbf{p}}|\mathcal{N}_{\mathbf{p}}\rangle = \sqrt{\mathcal{N}_{\mathbf{p}}}\mathcal{N}_{\mathbf{p}}\rangle, \quad \text{and} \quad \langle\langle \mathcal{N}_{\mathbf{p}}|b_{\mathbf{p}}^\dagger = \sqrt{\mathcal{N}_{\mathbf{p}}}\langle\langle \mathcal{N}_{\mathbf{p}}| \quad (15)$$

with

$$\langle\langle \mathcal{N}_p | \mathcal{N}_p \rangle\rangle = 1. \quad (16)$$

We consider the stimulated decay process of a pseudoscalar field in the coherent state $|\mathcal{N}_q\rangle\rangle$ into two photons via the four-momentum exchange: $q \rightarrow p_i + p_s$ under an inducing fields $|\mathcal{N}_{p_i}\rangle\rangle$ in the coherent state of photons accompanying generation of a signal photon p_s . The initial and final states, respectively, are thus defined as follows:

$$\begin{aligned} |\Omega\rangle &\equiv |\mathcal{N}_q\rangle\rangle |\mathcal{N}_{p_i}\rangle\rangle |0\rangle \quad \text{and} \\ \langle\Omega'| &\equiv \langle\langle \mathcal{N}_q | \langle\langle \mathcal{N}_{p_i} | \langle\langle 1_{p_s} | = \langle\langle \Omega | a_{p_s}. \end{aligned} \quad (17)$$

The transition amplitude is then expressed as follows

$$\begin{aligned} \langle\Omega' | S^{(1)} | \Omega\rangle &= \left(-\frac{1}{4} \frac{g}{M}\right) \frac{i^1}{1} \int d^4x (-i)^2 \times \\ &\int \frac{d^3\mathbf{s}}{(2\pi)^3 2s^0} \int \frac{d^3\mathbf{t}}{(2\pi)^3 2t^0} \langle\langle \mathcal{N}_{p_i} | \langle\langle 1_{p_s} | \\ &(S_{\mu\nu} \tilde{T}^{\mu\nu} e^{-i(s+t)x} a_s a_t + S_{\mu\nu} \hat{T}^{\mu\nu} e^{-i(s-t)x} a_t^\dagger a_s + \\ &\hat{S}_{\rho\sigma} \tilde{T}^{\rho\sigma} e^{-i(t-s)x} a_s^\dagger a_t + \hat{S}_{\rho\sigma} \hat{T}^{\rho\sigma} e^{i(s+t)x} a_s^\dagger a_t^\dagger | \mathcal{N}_{p_i}\rangle\rangle |0\rangle \times \\ &\int \frac{d^3\mathbf{u}}{(2\pi)^3 2u^0} \langle\langle \mathcal{N}_q | (e^{-iu_x} b_{\mathbf{u}} + e^{iu_x} b_{\mathbf{u}}^\dagger | \mathcal{N}_q\rangle\rangle. \end{aligned} \quad (18)$$

Results of photon annihilation-creation operators to the given states are summarized as follows

$$\begin{aligned} a_{\mathbf{k}} |\mathcal{N}_{p_i}\rangle\rangle |0\rangle &= \tilde{\delta}^3(\mathbf{k} - \mathbf{p}_i) \sqrt{N_{p_i}} |\mathcal{N}_{p_i}\rangle\rangle |0\rangle + |\mathcal{N}_{p_i}\rangle\rangle a_{\mathbf{k}} |0\rangle \\ &= \tilde{\delta}^3(\mathbf{k} - \mathbf{p}_i) \sqrt{N_{p_i}} |\mathcal{N}_{p_i}\rangle\rangle |0\rangle. \end{aligned} \quad (19)$$

$$a_l a_{\mathbf{k}} |\mathcal{N}_{p_i}\rangle\rangle |0\rangle = \tilde{\delta}^3(\mathbf{k} - \mathbf{p}_i) \sqrt{N_{p_i}} |\mathcal{N}_{p_i}\rangle\rangle a_l |0\rangle = 0 \quad (20)$$

because of $\mathbf{l} \neq \mathbf{k}$.

$$\begin{aligned} \langle\langle \mathcal{N}_{p_i} | \langle\langle 1_{p_s} | a_{\mathbf{k}}^\dagger &= \langle\langle \mathcal{N}_{p_i} | \langle\langle 1_{p_s} | \tilde{\delta}^3(\mathbf{k} - \mathbf{p}_i) \sqrt{N_{p_i}} + \\ &\langle\langle \mathcal{N}_{p_i} | \langle\langle 0 | \tilde{\delta}^3(\mathbf{k} - \mathbf{p}_s). \end{aligned} \quad (21)$$

$$\begin{aligned} \langle\langle \mathcal{N}_{p_i} | \langle\langle 1_{p_s} | a_{\mathbf{k}}^\dagger a_{\mathbf{l}}^\dagger &= \langle\langle \mathcal{N}_{p_i} | \langle\langle 0 | \tilde{\delta}^3(\mathbf{k} - \mathbf{p}_i) \sqrt{N_{p_i}} \tilde{\delta}^3(\mathbf{l} - \mathbf{p}_s) (22) \\ &+ \langle\langle \mathcal{N}_{p_i} | \langle\langle 0 | \tilde{\delta}^3(\mathbf{k} - \mathbf{p}_s) \tilde{\delta}^3(\mathbf{l} - \mathbf{p}_i) \sqrt{N_{p_i}} \end{aligned}$$

because of $\mathbf{l} \neq \mathbf{k}$. Combination of Eqs.(19) and (21) gives

$$\langle\langle \mathcal{N}_{p_i} | \langle\langle 1_{p_s} | a_{\mathbf{k}}^\dagger a_{\mathbf{l}} | \mathcal{N}_{p_i}\rangle\rangle |0\rangle = \tilde{\delta}^3(\mathbf{l} - \mathbf{p}_s) \tilde{\delta}^3(\mathbf{k} - \mathbf{p}_i) \sqrt{N_{p_i}}. \quad (23)$$

By substituting Eqs.(20),(22) and (23) into Eq.(18), we obtain the invariant amplitude kinematically consistent with the stimulated decay process: $q \rightarrow p_i + p_s$ as follows

$$\langle\Omega' | S^{(1_{dcy})} | \Omega\rangle = (-i)(2\pi)^4 \delta^4(q - p_i - p_s) \mathcal{M}_i \quad (24)$$

with

$$\mathcal{M}_i \equiv 2\sqrt{N_{p_i}} \sqrt{N_q} \left(-\frac{1}{4} \frac{g}{M}\right) \hat{P}_{i\rho\sigma} \hat{P}_s^{\rho\sigma} \quad (25)$$

and

$$\hat{P}_{i\rho\sigma} \hat{P}_s^{\rho\sigma} = \varepsilon^{\mu\nu\alpha\beta} p_{i\mu} p_{s\alpha} e_{i\nu}^* e_{s\beta}^* = -2\omega_i^2 \cos\Phi \quad (26)$$

where $\omega_i (= \omega_s) = m/2$ with $\omega_i \equiv p_i^0$ and $\omega_s \equiv p_s^0$ is the photon energy of the inducing field corresponding to half of the mass of a pseudoscalar particle, m , and Φ is a relative angle between the direction of the electric field component of the linear polarization of a decayed photon with respect to that of the magnetic field component of the linearly polarized inducing photons.

Given an invariant amplitude \mathcal{M} for the spontaneous decay rate of a rest particle with its four momentum p_0 and mass m into two photons : $p_0 \rightarrow p_1 + p_2$, the differential decay rate $d\Gamma$ is expressed as

$$d\Gamma = \frac{1}{2m} \frac{1}{2!} \int \frac{d^3\mathbf{p}_1}{(2\pi)^3 2\omega_1} \int \frac{d^3\mathbf{p}_2}{(2\pi)^3 2\omega_2} (2\pi)^4 \delta^4(p_1 + p_2 - p_0) |\mathcal{M}|^2 \quad (27)$$

where we introduced the factor of $1/2!$ because the two photons with energy ω_1 and ω_2 are identical particles. Then the differential rate with respect to a solid angle of p_1 is eventually expressed as

$$\frac{d\Gamma}{d\Omega_1} = \frac{|\mathcal{M}|^2}{128\pi^2 m}. \quad (28)$$

By substituting Eq.(26) into Eq.(25), we can express the invariant amplitude for the stimulated decay process as

$$\mathcal{M}_i = \sqrt{N_{p_i}} \sqrt{N_q} \left(\frac{g}{M}\right) \omega_i^2 \cos\Phi. \quad (29)$$

In order to equate \mathcal{M}_i in Eq.(29) with \mathcal{M} in Eq.(28), we must require that momentum and polarization of either one of decayed photons coincides with those of an inducing beam. This requirement originates from the delta function in the commutation relation in Eq.(8) as explicitly shown in the derivation of the amplitude. If a pseudoscalar particle exists at rest, p_1 and p_2 photons must be emitted back-to-back to each other with equal energies. Therefore, if p_1 photon in the spontaneous decay process coincides with p_i within a range of the inducing beam, the stimulated emission of p_2 , that is, the signal photon p_s must be exactly backward with respect to the p_1 direction. For later convenience, we define the induced decay rate as

$$\frac{d\Gamma_i}{d\Omega} \equiv N_i N_q \frac{d\Gamma_0}{d\Omega} \quad (30)$$

with

$$\frac{d\Gamma_0}{d\Omega} \equiv \frac{1}{128\pi^2 m} \left(\frac{g}{M}\right)^2 \omega_i^4 \cos^2\Phi \quad (31)$$

in order to factor out the field strength parameters.

Based on the above picture, we evaluate the stimulated reflection yield. For a laser field a Gaussian beam as a function of spacetime point (t, x, y, z) is typically used

to express a focused field [17]. We adopt the spherical wave propagation which is interpreted as the approximated wave propagation of a Gaussian beam at a far distance from the focal point [17]. Since in this case the wave front simply form a sphere, the entire solid angle of the inducing laser propagating from and to the focal point is available as the inducing decay area. Thus backward signal photons are, in principle, fully collectable at the incident point of the inducing field if dark matter particles are at rest with respect to the incident point, wherever signal photons are generated. This is thanks to the reversible nature of the coherent light propagation.

We consider the case in the upper part of Fig.1 where a pulsed inducing field with duration of τ is focused once and the searching beam is generated from the focal point. The central pulse position z of the inducing field is moving with the velocity of light c along the z -axis in free space which is occupied by coherent axions with the number density ρ_a . The stimulated reflection yield is then parametrized as follows

$$\mathcal{Y} = \int_{L_0/c}^{L_1/c} dt \int \rho_i dV_i \int \rho_a dV_i \int_0^{\Omega_i} \frac{d\Gamma_0}{d\Omega} d\Omega, \quad (32)$$

where V_i specifies the volume scanned by the inducing field while it propagates over the searching region from $z = L_0$ to L_1 with the solid angle $\Omega_i = \int_0^{\theta_0} d\theta \sin\theta \int_0^{2\pi} d\phi = 2\pi(1 - \cos\theta_0)$ defined by the divergence angle θ_0 determined by geometrical optics. The number density of the inducing field ρ_i is parametrized as $\rho_i(z) = \frac{N_i}{c\tau z^2 \Omega_i}$ as a function of z reflecting the situation that the pulse center position moves along the z -axis with the surface area of $z^2 \Omega_i$ at z . As for the volume integral on the axion density, we express it as $\mathcal{N}_q \equiv \int \rho_a dV_i = \int_{-\infty}^{\infty} dz' \rho_a c\tau z'^2 \Omega_i \delta(z' - z)$, where the delta function requires local overlaps with inducible ranges along the propagation of the inducing field. The stimulated reflection yield while the inducing field propagates is eventually estimated as

$$\begin{aligned} \mathcal{Y} &= \int_{L_0/c}^{L_1/c} dt \int_{L_0}^{L_1} dz z^2 \int_0^{\theta_0} d\theta \sin\theta \int_0^{2\pi} d\phi \frac{N_i}{c\tau z^2 \Omega_i} \times \\ &\quad \int_{-\infty}^{\infty} dz' \rho_a c\tau z'^2 \Omega_i \delta(z' - z) \frac{d\Gamma_0}{d\Omega} \Omega_i \\ &= \frac{L_1 - L_0}{c} N_i \cdot \rho_a \frac{2}{3} \pi (L_1^3 - L_0^3) \Omega_i \cdot \frac{d\Gamma_0}{d\Omega} \Omega_i \\ &= \frac{\pi}{48} \left[\frac{1}{m} \left(\frac{g}{M} \right)^2 \omega_i^3 \right] \times \\ &\quad \left(\frac{L_1 - L_0}{c} \frac{c}{\lambda_i} \right) \cos^2 \Phi N_i \rho_a (L_1^3 - L_0^3) (1 - \cos\theta_0)^2 \end{aligned} \quad (33)$$

where the factor enclosed by [] partially keeps natural units while ω_i out of ω_i^4 in Eq.(31) is replaced with frequency using the wavelength of the inducing field λ_i . It

is important to note that the stimulated reflection yield eventually does not depend on whether the inducing field is provided as a pulsed wave or a continuous wave.

As the inducing field in the coherent state, we consider broad-band pulsed lasers since target axions in this paper are in the eV mass range. In order to scan a wide mass range, pulsed lasers from the optical comb [18] would be useful. In the following evaluation we assume availability of optical comb covering $0.35 \mu\text{m} - 4.4 \mu\text{m}$ [18] by assuming a flat wavelength spectrum for simplicity.

We provide sensitivity evaluations in the following two experimental approaches: A) a laboratory based experiment targeting on the mean number density of axions around the Sun as cold dark matter [19], B) a remote detection aiming at the locally concentrated number density in hair-roots due to the gravitational lensing effect by Earth. We thus introduce the local concentration factor C as follows

$$\rho_a \sim C \frac{0.4 \times 10^9 \text{ [eV/cm}^3\text{]}}{m \text{ [eV]}}. \quad (34)$$

The local velocity of cold dark matter on Earth is traditionally assumed to follow the Maxwellian velocity distribution by taking the Sun's velocity is stationary with respect to the average velocity of cold dark matter [15]. However, there should also be a fraction of cold dark matter whose velocity distribution has non-thermal natures [20]. In A) with $C = 1$, we thus conservatively assume that dark matter particles are moving with the escape velocity from the Galaxy $\sim 300 \text{ km/s}$ [19] at maximum to any observation points, that is, the maximum relative velocity of $\beta = \mathcal{O}(10^{-3})$ in units of the velocity of light c . In order to allow deviations of induced emission angles from the exact backward direction due to the slight transverse Lorentz boost, the radius of the signal collector, R_c , must satisfy $R_c \sim \beta L_1$ with the depth of the searching volume L_1 . Therefore, if $R_c = 1 \text{ m}$ is assumed, the searchable depth is limited to $L_1 \sim 10^3 \text{ m}$. In this case the acceptance factor to all of signal photons can be $A_{cc} \sim 1.0$.

In B) with $C = 10^7 - 10^9$, we consider shooting a coherent pulsed inducing beam to a remote cold dark matter target such as concentrated dark matter hair-roots localized at around 10^9 m from Earth [15]. Since these dark matter hair-roots originate from the gravitational lensing effect by Earth, the target should be comoving with Earth. As illustrated in Fig.1, instead of observing signal photons on the ground, the most ideal location of the laser injection and the signal photon detector would be the \mathcal{L}_2 point, $1.5 \times 10^9 \text{ m}$ from Earth, known as one of five Lagrange points which is on the straight line between the Sun and Earth. This is because the detection system can be contained within the shadowed volume by Earth allowing for mitigating background photons from the Sun and also absorption of signal photons in the air. The length of a hair-root is estimated by using Eq.(36) in [15]

where the focal length F for cold dark matter streams incident with the velocity $v = 220$ km/s as a function of the impact parameter b is expressed as $F(b) = \frac{\xi R_E^2}{3} (1 + \frac{b^2}{4R_E^2})$ with $\xi \equiv v^2/(GM_E) = 1.2 \times 10^{-4} \text{ m}^{-1}$, Earth's radius R_E and mass M_E , and the gravitational constant G . By changing b from 0 to R_E , the expected hair-root range from $L_0 = (1.6-1.5) \times 10^9$ m to $L_1 = (2.1-1.5) \times 10^9$ m is obtained where the offset is the location of \mathcal{L}_2 . We conservatively take a constant $C \sim 10^7$ over the hair-root range. Given $F(b = R_E) = 5\xi R_E^2/12$, the indent angle of dark matter streams at the focal point is estimated as $\sim R_E/F(b = R_E) = 12/(5\xi R_E) = 3.1 \times 10^{-3}$ rad. Therefore, the transverse velocity in units of c in a focused hair-root with respect to the propagation direction of the inducing beam is estimated as $\beta = 2.3 \times 10^{-6}$ given the incident velocity $v = 220$ km/s. It is practically impossible to collect all of signal photons in this case. The acceptance factor of the signal collector with the radius $R_c = 1$ m is estimated as $A_{cc} \sim (R_c/(\beta L_1))^2 = 6.2 \times 10^{-7}$.

In the both approaches, we consider measuring the arrival time distribution of signal photons with the orthogonally rotated linear polarization state to the linear polarization direction of the inducing laser by requiring the same photon energy as that of the inducing laser. We assume a single photon sensitive device such as a photomultiplier whose random thermal noise rate can be typically suppressed at $r_{thn} = 1$ Hz. The overall signal collection factor including the detection efficiency is assumed to be $\epsilon = 0.1A_{cc}$. The repetition rate of the inducing pulse laser is assumed to be $f = 1$ Hz. Within the scanning time window of $(L_1 - L_0)/c$ per shot, the accidental coincidence rate between the thermal noise rate and the laser repetition rate is expressed as $R_{bkg} \equiv 2r_{thn}f(L_1 - L_0)/c$. We thus can discuss a null hypothesis as Gaussian fluctuations after subtracting the total background statistics TR_{bkg} with the data acquisition time $T = 10^6$ sec from the observed number of photons consistent with the signal feature. In order to evaluate the sensitivity, we require that the observed yield $fT\epsilon\mathcal{Y}$ based on Eq.(33) is greater than five standard deviations of the subtraction-associated fluctuation over the total statistics, that is, $\delta N_{bkg} = 5\sqrt{2TR_{bkg}}$. Therefore, the upper limit of the coupling strength when no signal photon is observed is expressed as

$$\frac{g}{M} = \sqrt{\frac{\delta N_{bkg}}{fT\epsilon \frac{\pi\omega_i^3}{48m} \left(\frac{L_1 - L_0}{\lambda_i}\right) N_i \rho_a (L_1^3 - L_0^3) (1 - \cos \theta_0)^2}} \quad (35)$$

by requiring the orthogonal polarization state $\cos \Phi = 1$.

The magenta solid and dashed horizontal curves in Fig.2 show expected reachable coupling strengths obtained from Eq.(35) for A) and B), respectively, as a function of axion mass $m = 2\omega_i$ covered by the laser spectrum range. For simplicity we commonly assume the inducing laser pulse energy of 1 J and the diver-

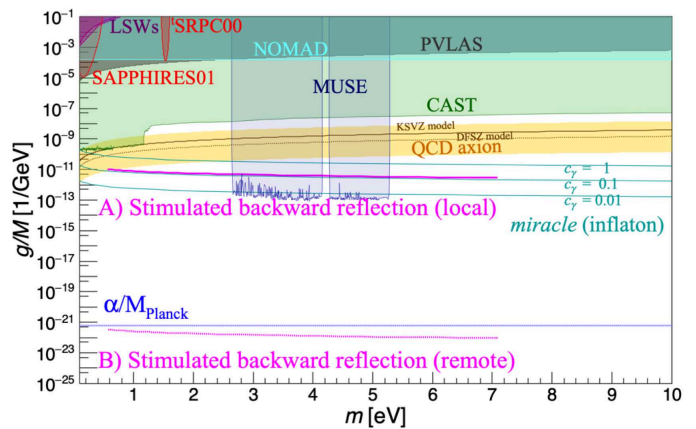


FIG. 2: Sensitivity projections based on backward reflection from stimulated axion decay by surveying with a spherical inducing laser field. The details of symbols and used parameters can be found in the main text.

gence angle at the incident points, $\theta_0 = 1$ mrad. The range of photon wavelengths is $\lambda_i = 0.35 - 4.4 \mu\text{m}$. The searching depths of $L_0 = 0 \sim L_1 = 10^3$ m and $L_0 = 0.1 \times 10^9 \sim L_1 = 0.6 \times 10^9$ m are assumed for A) and B), respectively. The upper solid brown line and yellow band are the predictions from the benchmark QCD axion model: the KSVZ model [21] with the model parameters $E/N = 0$ and with $0.07 < |E/N - 1.95| < 7$, respectively, while the bottom dashed brown line is the prediction from the DFSZ model [22] with $E/N = 8/3$. The cyan lines are the predictions from the ALP *miracle* model relevant to inflation[13] with the model parameters $c_\gamma = 1, 0.1, 0.01$. The gray area shows the excluded region by the vacuum magnetic birefringence experiment (PVLAS [23]). The purple areas are excluded regions by the Light-Shining-through-a-Wall (LSW) experiments (ALPS [24] and OSQAR [25]). The light-cyan horizontal solid line indicates the upper limit from the search for eV (pseudo)scalar penetrating particles in the SPS neutrino beam (NOMAD) [26]. The blue areas are exclusion regions from the optical MUSE-faint survey [28]. The green area indicates the excluded region by the helioscope experiment CAST [29]. The red shaded area shows the excluded range based on a stimulated resonant photon collider, SRPC, in quasi-parallel collision geometry (SAPPHIRES01) [30]. The red filled area indicates the excluded range by a pilot search with the fixed angle three-beam SRPC(*SRPC00) [31].

In conclusion, we have formulated the stimulated decay process of a pseudoscalar particle into two photons in the background of an inducing coherent electromagnetic field and applied the formula to obtain the stimulated backward reflection yield based on the spherical wave propagation of the inducing laser field. For the laboratory based experiment targeting on locally mov-

ing cold dark matter, the sensitivity can reach $f_a \sim 10^7$ GeV, for instance, based on the concrete relation $g/M = \alpha/(2\pi f_a)C_\gamma = 1.2 \times 10^{-11}$ GeV $^{-1}$ with $C_\gamma = 0.1$ in the model [9]. We also have evaluated the yield in the ideal case where an observer stays at \mathcal{L}_2 Lagrange point so that positions of dark matter hair-roots can be stationary with respect to \mathcal{L}_2 . The 4th power dependence on the search depth of the signal yield can significantly improve the sensitivity to the weak coupling domain. This evaluation indeed indicates very high sensitivity even beyond the gravitational coupling strength $\alpha/M_{Planck} = 6 \times 10^{-22}$ GeV $^{-1}$.

We have focused on the eV mass range as the concrete application of the proposed method in this paper, however, the method is in principle extendable to any frequency ranges of inducing beams. Given intense coherent photon sources over many orders of magnitude in frequency, it is also in principle possible to perform B)-type experiments from the ground, since locations of reflection signals are predictable based on the rotation speed of Earth at the detector location, though the air and clouds become obvious background sources. However, if time-of-flight is properly combined with pulsed inducing fields, we can separate long-traveled reflection signals from the distant dark matter target against such short distance background components. In practice, ground based experiments have advantage in capability of supplying high power to the sources. Once we could identify axion mass, this method can also provide a measure for local and remote dark matter velocity distributions based on divergence angles of reflected signal photons.

ACKNOWLEDGMENTS

The author acknowledges Tomohiro Inagaki, Taiyo Nakamura and Tsunefumi Mizuno for useful discussions and also the support of the Collaborative Research Program of the Institute for Chemical Research at Kyoto University (Grant Nos. 2018–83, 2019–72, 2020–85, 2021–88, 2022–101, and 2023–101) and Grants-in-Aid for Scientific Research Nos. 17H02897, 18H04354, 19K21880, and 21H04474 from the Ministry of Education, Culture, Sports, Science and Technology (MEXT) of Japan.

[1] R. D. Peccei and H. R. Quinn, “CP Conservation in the Presence of Instantons”, *Phys. Rev. Lett.* **38**, 1440-1443 (1977) doi:10.1103/PhysRevLett.38.1440.
 [2] R. D. Peccei and H. R. Quinn, “Constraints Imposed by CP Conservation in the Presence of Instantons”, *Phys. Rev. D* **16**, 1791-1797 (1977) doi:10.1103/PhysRevD.16.1791.
 [3] S. Weinberg, “A New Light Boson?”, *Phys. Rev. Lett.* **40**, 223-226 (1978) doi:10.1103/PhysRevLett.40.223.

[4] F. Wilczek, “Problem of Strong P and T Invariance in the Presence of Instantons”, *Phys. Rev. Lett.* **40**, 279-282 (1978) doi:10.1103/PhysRevLett.40.279.
 [5] J. Preskill, M. B. Wise and F. Wilczek, “Cosmology of the Invisible Axion”, *Phys. Lett. B* **120**, 127-132 (1983) doi:10.1016/0370-2693(83)90637-8.
 [6] M. Dine and W. Fischler, “The Not So Harmless Axion”, *Phys. Lett. B* **120**, 137-141 (1983) doi:10.1016/0370-2693(83)90639-1.
 [7] L. F. Abbott and P. Sikivie, *Phys. Lett. B* **120**, 133-136 (1983) doi:10.1016/0370-2693(83)90638-X.
 [8] L. Di Luzio, F. Mescia, E. Nardi, P. Panci and R. Ziegler, “Astrophobic Axions,” *Phys. Rev. Lett.* **120**, no.26, 261803 (2018) doi:10.1103/PhysRevLett.120.261803 [arXiv:1712.04940 [hep-ph]].
 [9] M. Badziak and K. Harigaya, “Naturally astrophobic QCD axion”, *JHEP* **06**, 014 (2023) doi:10.1007/JHEP06(2023)014 [arXiv:2301.09647 [hep-ph]].
 [10] G. G. Raffelt, J. Redondo and N. Viaux Maira, “The meV mass frontier of axion physics”, *Phys. Rev. D* **84**, 103008 (2011) doi:10.1103/PhysRevD.84.103008 [arXiv:1110.6397 [hep-ph]].
 [11] M. Giannotti, I. Irastorza, J. Redondo and A. Ringwald, “Cool WISPs for stellar cooling excesses”, *JCAP* **05**, 057 (2016) doi:10.1088/1475-7516/2016/05/057 [arXiv:1512.08108 [astro-ph.HE]].
 [12] M. Giannotti, I. G. Irastorza, J. Redondo, A. Ringwald and K. Saikawa, “Stellar Recipes for Axion Hunters”, *JCAP* **10**, 010 (2017) doi:10.1088/1475-7516/2017/10/010 [arXiv:1708.02111 [hep-ph]].
 [13] Ryuji Daido et al., “The ALP miracle revisited”, *Journal of High Energy Physics*, 02 (2018) 104, 16th February 2018.
 [14] P. Sikivie, “Experimental Tests of the “Invisible” Axion”, *Phys. Rev. Lett.* **51**, 1415 (1983) and *Erratum ibid.*, **52**, 695 (1984).
 [15] G. Prézeau, “Dense Dark Matter Hairs Spreading Out from Earth, Jupiter and Other Compact Bodies,” *Astrophys. J.* **814**, no.2, 122 (2015) doi:10.1088/0004-637X/814/2/122 [arXiv:1507.07009 [astro-ph.CO]].
 [16] R. J. Glauber, “Coherent and Incoherent States of the Radiation Field”, *Phys. Rev.* **131** (1963), 2766.
 [17] Amnon Yariv, *Optical Electronics in Modern Communications* Oxford University Press (1997).
 [18] Kana Iwakuni et al., “Generation of a frequency comb spanning more than 3.6 octaves from ultraviolet to mid infrared”, *Optics Letters* **41** 3980 (2016). <http://dx.doi.org/10.1364/OL.41.003980>
 [19] Y. Sofue, “Rotation Curve of the Milky Way and the Dark Matter Density,” *Galaxies* **8**, no.2, 37 (2020) doi:10.3390/galaxies8020037 [arXiv:2004.11688 [astro-ph.GA]].
 [20] P. Sikivie, I. I. Tkachev and Y. Wang, “The Velocity peaks in the cold dark matter spectrum on earth,” *Phys. Rev. Lett.* **75**, 2911-2915 (1995) doi:10.1103/PhysRevLett.75.2911 [arXiv:astro-ph/9504052 [astro-ph]].
 [21] J. E. Kim, *Phys. Rev. Lett.* **43**, 103 (1979); M. Shifman, A. Vainshtein, and V. Zakharov, *Nucl. Phys. B* **166**, 493 (1980).
 [22] M. Dine, W. Fischler, and M. Srednicki, *Phys. Lett.* **104B**, 199 (1981); A. Zhitnitskii, *Sov. J. Nucl. Phys.* **31**, 260 (1980).

- [23] A. Ejlli *et al.*, *Physics Reports* 871 (2020) 1 201374.
- [24] K. Ehret *et al.* (ALPS), *Phys. Lett. B* **689**, 149 (2010).
- [25] R. Ballou *et al.* (OSQAR), *Phys. Rev. D* **92**, 9, 092002 (2015).
- [26] P. Astier *et al.* (NOMAD), *Phys. Lett. B* 479 (2000) 371-380.
- [27] A. Ayala *et al.*, *Phys. Rev. Lett.* 113, 19, 191302 (2014).
- [28] Marco Regis, Marco Taoso, Daniel Vaz, Jarle Brinchmann, Sebastiaan L. Zoutendijk, Nicolas F. Bouché, Matthias Steinmetz, *Physics Letters B*, 814 (2021) 136075.
- [29] V. Anastassopoulos *et al.* (CAST), *Nature Phys.* **13**, 584 (2017).
- [30] Y. Kirita *et al.* [SAPPHIRES], “Search for sub-eV axion-like particles in a stimulated resonant photon-photon collider with two laser beams based on a novel method to discriminate pressure-independent components,” *JHEP* **10**, 176 (2022) doi:10.1007/JHEP10(2022)176 [arXiv:2208.09880 [hep-ex]].
- [31] F. Ishibashi, T. Hasada, K. Homma, Y. Kirita, T. Kanai, S. Masuno, S. Tokita, M. Hashida, ”Pilot search for axion-like particles by a three-beam stimulated resonant photon collider with short pulse lasers”, *Universe* 2023, 9(3), 123.